

Heat Transfer Analysis of Conventional Round Tube and Microchannel Condensers in Automotive Air Conditioning System

Muayad Abdulnabi*

Department of Mechanical Engineering, University of Baghdad, Baghdad, Iraq

Asst. Prof. Issam Mohammed

Department of Mechanical Engineering, University of Baghdad, Baghdad, Iraq

Abstract

In this paper, an experimental analysis of conventional air cooled round tube and microchannel condensers in an automotive air conditioning cycle in term of heat transfer coefficient and energy is presented. The analysis was carried out in a test unit of automotive air conditioning system works with R134a. The conventional round tube plate fin condenser, and cycle were examined first. After that the conventional condenser is replaced by a parallel flow multi-louvered fin microchannel condenser with 0.1 mm hydraulic diameter, and the same experiments in same conditions have been re-implemented. The performance of two condenser and cycles were tested in terms of ambient temperature, which it was varied from 40°C to 65°C. Besides, the indoor temperature and load has been set to 23°C and 2200 W respectively. It was found that replacing the round tube conventional condenser with a microchannel is useful and can enhances the total cycle performance. Because, the microchannel condenser has 224 % and 77 % higher refrigerant side and air side heat transfer coefficient than the conventional. So that, the COP, in case of using the microchannel condenser, was found to be 20 % higher than the conventional. In addition, the microchannel condenser 50 % smaller volume than the conventional. Therefore, it provides more empty space in the car engine container to be occupied with other components or to be removed.

Keywords: Automotive air conditioning, Condenser, Microchannel, Heat transfer, Energy

1. Introduction

One of the basic problems in the refrigeration cycle, specifically the one containing an air cooled condenser, is the high condensing temperature. The condensing temperature may rise due to the increased temperature of the environment. In fact, the vapor compression refrigeration cycle (VCRC) will suffered from a reduction in performance when the ambient temperature increases. Because, with rising temperature, the compressor discharge pressure increases due to the reduction in heat sink ability in receiving heat. The increased discharge pressure resulting in high compressor work, low refrigeration effect, and thus low coefficient of performance. Now, a new solution may be the key of designing a very effective heat exchanger, including the condenser, even for high ambient temperature, is by using a new type of a very compact heat exchanger. Or, what is commonly known as the microchannels heat exchangers. According to Kandlikar and Grande [1], the microchannels is the channels with hydraulic diameter from 10 μm to 200 μm . While Mehendale et.al [2] define it to be from 1 μm to 100 μm hydraulic diameter. Other studies [3] consider the fluid flow behavior inside the microchannel to construct the definition. The microchannel condensers usually designed with a multiport parallel tube arrangement and multi-louvered fin. Furthermore, the multiport tubes inside the main tube can have different shapes. The microchannels have an increasingly applications as future alternatives for the traditional heat exchangers and also in the medical applications [4]. A lot of studies are made investigate the heat transfers throughout the microchannel condenser and its effect on the refrigeration cycle. Park and Hrnjak [5] carried out a comparison of performance between a prototype microchannel condenser and a traditional condenser. The experiments take place in a residential air conditioning system with refrigerant R410A, in order to test the microchannel condenser effect on cycle performance. The two condensers made of exactly the same face area, external volume and fins density. But, the conventional condenser is round tube with 9.5 mm outside diameter while the microchannel condenser is rectangular with 1.9 \times 21 mm. The results show that the use microchannel condenser leads to improve the cycle performance as well as condenser and evaporate capacities for the same operation conditions. Also, they found that, the use of microchannel condenser leads to have 9 % reduction in refrigerant charge. Shah [6] investigated the condensation inside mini and microchannels by the use of his own well-verified correlation [7]. The correlation showed to have 500 correct predictions for 15 experiments for the same functional parameters which were: the reduce pressure from 0.048 to 0.52, the hydraulic diameter from 0.49 mm to 5.3 mm and the mass fluxes from 50 to 1400 $\text{kg/m}^2\text{s}$ for 8 different fluid condensate inside rectangular and round tubes for both the single port and multiport channels. The correlation has 15.9 mean error from the experiments. The correlation is found to be in a good agreement with 15 study for round and multiport tubes and with hydraulic diameter from 0.49 mm to 5.3 mm. H.S. Wang and John W. Rose [8] presented a theoretical model for condensation inside microchannels. The model takes into consideration the gravity effect, the shear stress on the surface of the condensate fluid, the pressure gradient caused by the surface tension and the

effect of channel inclination. The analysis carried out for different channel shapes, dimensions, vapor mass velocity and various temperature differences between the surface and the vapor. They found that, for the microchannels, the vapor local parameters cannot be measured directly without uncertainties in values. But, nevertheless, it can be measured with less inaccuracy by calculating the parameters at the inlet and the outlet of the microchannel. Also, they found that for all the fluids, channel configuration and mass flux, the heat flux for the same temperature difference between the vapor and the surface is constant. Which means that, the heat flux is indented of the channel area and fluid mass flow rate. Kim and Mudawar [9] examined the heat transfer coefficient and the pressure drop characteristics for condensation inside rectangular microchannel. A theoretical control volume is present for FC-72 based the smooth interface between the vapor region and the annular liquid film which is assumed to be uniform all over the perimeter of the microchannel. An experimental work was carried out to test the validity of the theoretical model. The experimental work includes two cycles for the major working fluid which is the FC-27 and the other for the secondary fluid which is water uses to collect the heat from the microchannel condenser. Moreover, the experimental work is done by 24 individual experiment for various mass fluxes and for four distinctive water flow rate. The model was compared with other data points for other studies and it shows a good convergence with them. Kim and Mudawar [10] developed two general correlations for the condensation heat transfer coefficient inside mini/microchannel for different substances, properties, geometries and flow parameters. They found their new correlations by curve fitting of a large database of 4045 points from 28 sources for 1964 data for single-channel, 2081 data for multi-channel, 0.424-6.22 mm hydraulic diameter, 53-1403 kg/m²s mass fluxes and only for smooth surfaces. These two new correlations are proposed for annular, slug and bubbly flows and they showed good predictions with an overall error of 16 %. AL-Hajri et.al [11] carried out an experimental examination for condensation inside microchannels. So as to explore the effect of mass flux, condenser saturation temperature and inlet degree of superheat on the heat transfer coefficient and pressure drop features in a rectangular microchannel condenser. The microchannel condenser has 0.4×2.88 mm a cross section area, 190 mm long, 7:1 aspect ratio, 0.7 mm hydraulic diameter, 6.4 mm wetted perimeter and 2 mm thickness. The experiments executed for two refrigerant R134a and R245fa for different domains of tested parameters which were; 50-500 kg/m²s mass flux, 30-70°C saturation temperature, 0-15°C degree of inlet super heat and 7-115 W cooling load. They found that, the heat transfer coefficient as well as the pressure drop are powerful functions of mass flux and saturation temperature, both of them are increasing with the increment of mass flux while they are decreasing with saturation temperature. In contrast with the inlet degree of superheat which shown to have no considerable effect neither on heat transfer coefficient nor the pressure drop. G. Goss and J.C. Passos [12][13] investigated the local heat transfer coefficient and the pressure drop experimentally during the condensation of R134a inside eight parallel microchannels with 0.77 mm diameter. The parameters under test were; the refrigerant mass flux from 230 to 445 kg/m²s, pressure from 7.3 to 9 bar, heat flux from 17 to 35 kW/m² and vapor quality from 0.55 to 1. They found that, the mass flux and the dryness fraction has the greatest influence on the heat transfer coefficient than the other parameters. Also, they found that the resistance of the heat transfer is mainly caused by the film weak conduction especially at 0.95 dryness fraction. For the pressure drop, it is found to be increased with the mass velocities and decreased with the increment of the saturation temperature. Besides, 95 % of the loss in the pressure is caused by the friction. Huang et.al [14] provided an air to refrigerant model based on the finite volume method to simulate the condensation in microchannels. The model is made for multiple tube and fin shapes so as to provide the most adaptive geometry which enhance the thermal performance and reduce cost. The model showed very well effectiveness for 227 data points of several experiments include eight different working fluid as well as four various geometries. Their results showed that the average rate of perversion from the measured values of the heat transfer coefficient as well as the pressure drop for a configuration and operating conditions are 2.7 % and 28 % respectively. X. Yin et al. [15] developed a numerical model for a microchannel condenser based on the finite volume method. Their model includes some factors of great influence on the condenser which is; the non-uniform air temperature, the refrigerant maldistribution through the tubes, the face velocity, fin conductivity and the air side distribution for one and two slabs microchannel condenser. They found that the asymmetric air flow effect the performance of the condenser by 1.5 % for the heat transfer, 6.8 % for the pressure drop and 12.5 % for the refrigerant charge in the one slab microchannel condenser. While, for the two slabs it is affecting the performance overall by 0.5 % for the capacity and 9.7 for the pressure drop. Also, they found that the fin conductivity in the transverse section effect slightly by 0.06 % for the capacity and 0.16 % for the pressure drop

2. Experimental Facilities and Condensers Description

The test rig is an automobile air conditioner training unit operating with refrigerant R134a. It includes the complete car air conditioner fitted on a wheeled steel frame together with the driving motor. The unit is composed of the following components: multi cylinder compressor with electromagnetic clutch, forced air condenser, evaporator with multispeed fan, liquid receiver and filter drier, thermostatic expansion valve, pressure switch and connection hoses. A schematic diagram of the test rig is shown in Figure 1, while Table 1 provides

general specifications of it. Moreover, the test rig is a simulation of the car air conditioning system. So that, the device is consisting of two separate compartments: the passengers' compartment and the environment compartment. The passengers' compartment is insulated from the surrounding and from the environment compartment by a glass layer to represent the car glass windows. The passengers compartment contains the evaporator, an electrical heater to simulate the load inside the compartment and the thermostatic expansion valve, while environment compartment contains the compressor, the electrical motor, the condenser and the filter drier.

Figure 2 shows a photograph of the two condensers while Figure 3 and 4 show a geometrical diagram of microchannel and the conventional round tube condensers respectively. Besides, Table 2 and 3 provide the technical data of the microchannel and conventional round tube condensers respectively. Due to limitations in manufacturing, the microchannel condenser has different areas from the baseline round tube condenser as it shown in Table 4. The condenser (the round tube or the microchannel) is, fitted to the main frame by screw connections and it is supplied with an axial fan that works with the cycle to increase the air flow rate when the condensation temperature rises. The condenser fan controlled by the pressure switch that it starts at 15 bar and stops at 12 bar.

3. Heat Transfer Analysis

During the analysis, the following assumptions have been adopted:

1. Steady state.
2. Constant mass flow rate throughout the all parts.
3. No heat loss through the rubber tubes.
4. All the condenser external area considered as a finned surface because ($A_f \gg A_{un-f}$).
5. The conduction resistance is very low that can be neglected.
6. The fouling resistance in both condensers is negligible.

The EES program is used to solve the mathematical model which can be presented as follows; Firstly, the air side heat transfer coefficient can be found, experimentally, by equating the heat rate obtained from the temperature rise of the air, to the heat rate obtained by the convection. But, initially, the air properties are calculated at an average air temperature given by:

$$T_{av,a} = \frac{T_{R,i} + T_{a,i}}{2} \quad (1)$$

Where $T_{av,a}$ is the average air temperature in (K), $T_{R,i}$ is the refrigerant temperature at condenser inlet in (K) and $T_{a,i}$ is the air inlet temperature in (K).

The air mass flow rate is given by:

$$\dot{m}_a = \rho_a * V_a * A_c \quad (2)$$

Where \dot{m}_a is the air mass flow rate in (kg/s), ρ_a is the air density in (kg/m³). V_a is the air velocity in (m/s).

The heat transfers to the air due to the temperature rise is given by:

$$Q_a = \dot{m}_a * c_{p_a} * (T_{a,o} - T_{a,i}) \quad (3)$$

Where Q_a is the heat transferred to the air in (W), c_{p_a} is the air specific heat in (J/kg.K) and $T_{a,i}$ and $T_{a,o}$ are the inlet and the outlet temperatures respectively, in (K).

Now, by using assumption (4), the heat transferred to the air due to the convection on the outer surface, is given by

$$Q_a = h_a * A_o * \eta_o (T_w - T_{a,i}) \quad (4)$$

Where h_a is the air side heat transfer coefficient in (W/m².K), T_w is the average tube wall temperature in (K) and η_o is the overall surface efficiency and it is given by:

$$\eta_o = 1 - \frac{A_f}{A_o} (1 - \eta_f) \quad (5)$$

Where A_f is the fin area in (m²), A_o is the outer convection area in (m²) and η_f is the fin efficiency, which can be found by unitizing the EES built-in functions (Fin Efficiency functions). The **Annular Rectangular Fin** procedure is used. This procedure requires the value of the equivalent effective fin radius, which it's given by [16]

$$r_{f,eff} = \sqrt{\left(A_f * \frac{p_f}{2\pi L_t} + \left(\frac{D_o}{2} \right)^2 \right)} \quad (6)$$

Where $r_{f,eff}$ is the effective fin radius in (m), p_f is the fin pitch in (m), L_t is the tube length in (m) and D_o is the

outside diameter of the tube in (m).

The evaluation of the fin efficiency in EES requires the air side heat transfer coefficient value. But this value cannot be determined without equation 4. Thus, a trial and error method of solution is carried out. The iteration starts with a guess value of the air side heat transfer coefficient. The guess value and the effective fin radius obtained by equation 6, are used to calculate the fin efficiency by the EES built-in functions. The fin efficiency is substituted into equation 5 to find the overall surface efficiency. The guess value and the overall surface efficiency are substituted in equation 4 to find the heat transfer rate. The guess value is updated until equation 4 becomes equal to equation 3. The equality of the two equations gives the true value of the air side heat transfer coefficient. After calculating the air side heat transfer coefficient, the air side resistance to the heat transfer is given by [16]

$$R_a = \frac{1}{h_a A_o \eta_o} \quad (7)$$

Where R_a is the air side resistance in (K/W).

The refrigerant side heat transfer coefficient can be determined as average for the total condenser length regardless from the condenser zones. Thus, in this section, the equations for such calculations will be presented, while the heat transfer coefficient of each section of condenser will be given in the next section. Now, this methodology of calculating the refrigerant side heat transfer coefficient as average, starts by estimating the total heat transfer resistance, which can be written as [17]:

$$R_{total} = \frac{T_{R,s} - T_{a,i}}{Q_H} \quad (8)$$

Where R_{total} is the total resistance in (K/W) and $T_{R,s}$ is the condensing temperature in (K).

By using assumption (5) and (6), the total resistance is a sum of the refrigerant side resistance and the air side

$$R_{total} = R_R + R_a \quad (9)$$

Where R_R is the refrigerant side resistance in (K/W), and it can be written as [17]

$$R_R = \frac{1}{h_R A_i} \quad (10)$$

Where h_R is the refrigerant side heat transfer coefficient in (W/m²K).

Substituting equation 10 into 9 and rearranging to obtain a direct expression of the refrigerant side heat transfer coefficient:

$$h_R = \frac{1}{A_i} * \frac{1}{R_{total} - R_a} \quad (11)$$

4. Results and Discussion

The results have been obtained after solving the previous equations by the EES program. The ranges of operational conditions are given in Table 5.

Figure 5 shows that the refrigerant side heat transfer coefficient of the microchannel condenser is about 224 % higher than the conventional. This increment can be explained by the higher mass flux that the microchannel works with. The higher mass flux resulted mainly from the smaller flow area that caused by the very small hydraulic diameter of the microchannel condenser (0.1 mm). In fact, the conventional condenser works with 200 kg/m²s mass flux, while the microchannel works with 787 kg/m²s. Thus, the microchannel mass flux is larger in about 294 % than the conventional. Thus, since the refrigerant side heat transfer coefficient has a direct proportion with the mass flux, it will be higher also.

Figure 6 shows that the microchannel has 5 % larger heat rejection than the conventional. Also, this is due to the higher refrigerant side and air side heat transfer coefficients that the microchannel works with. However, it must be noted that, although the microchannel condenser has 224 % larger heat transfer coefficient than the conventional, the difference in heat rejection is only 5 %. But, this ratio is due to the fact that; the convection area has a direct proportion with heat transfer rate. Thus, the smaller the area, the smaller the heat transfer rate. However, the conventional round tube condenser has 0.2156 m² internal convection area, while the microchannel has 0.08 m². So that, it has 170 % larger internal convection area than the microchannel. Therefore, the increment in heat transfer coefficient, in case of using microchannel condenser, is accompanied by a decrement in convection area. That, if heat transfer coefficient increased by half for example, and the convection area decreased by half, they will cancel each other out and the same rate of heat transfer will be obtained for the same temperature difference. This fact can be seen by the ratio of (hA) product, which is

$$\frac{(hA)_{\text{Microchannel}}}{(hA)_{\text{conventional}}} = \frac{4174 * 0.08}{1318 * 0.2156} = 1.17 \quad (12)$$

Where 4174 and 1318 are the average refrigerant side heat transfer coefficient for the microchannel cycle and the conventional respectively. So, the increment in heat rejection should be 17 % not 5 % if the temperature difference assumed to be the same in both condensers. But, due to limitation in measuring system, the difference in temperature between the fluid and the internal wall is not measured. Also, the microchannel condenser is made from aluminum, while the conventional is made from copper. So that the microchannel has 20 % lower thermal conductivity than the conventional as average. Thus, since the thermal conductivity is different, the same temperature difference is not expected to occur. And, the missing 12 % of heat rejection may be due to the expected lower temperature different that the microchannel condenser works with. Nonetheless, this 12 % could also due to some error in experiments, or due to the behave of heat transfer rate and coefficient with ambient temperature and condenser air speed. Finally, it must be noted that the refrigerant side heat transfer coefficient and even the air side, are practical functions, which depend on large of parameters contribute together to produce the heat transfer coefficient. In fact, these parameters are not increase or decrease gradually or simultaneously. But, instead of that, they change in a different ranges resulted, sometimes, in a nonlinear behavior of heat transfer coefficient. So, although this case didn't exactly happen, but it may give some justifications for points that out of the expected curve behavior which may causes a fluctuation in the difference ratio of heat transfer coefficient.

Figure 7 shows that the air side heat transfer coefficient of the microchannel condenser is about 77 % larger than the conventional. This ratio is due to the difference in fin configuration since the conventional condenser fins are wavy fins, while the microchannel fins are multi-louver fins. So, this higher air side heat transfer coefficient of microchannel condenser resulted the air side heat gain to be 10 % higher than the conventional as shown in Figure 8. Again, it seems that the ratio of air side heat gain increment is so small comparing with that of heat transfer coefficient. But, this ratio is caused by the smaller external convection area of the microchannel and the fewer temperature difference as well. Because the microchannel condenser has 7.14 m² external convection area, while the conventional has 8.942 m². That means 20 % reduction in external area. Also, the average temperature difference between the wall and the inlet air is found to be 14.5°C and 18.5°C for the microchannel condenser and the conventional respectively. Therefore, the temperature difference in reduced by 22 %. So, by substituted these numbers into the equation of heat transfer ratio, it was found:

$$\frac{Q_{\text{Microchannel}}}{Q_{\text{conventional}}} = \frac{hA\Delta T}{hA\Delta T} = \frac{48}{27} * \frac{7.14}{8.942} * \frac{14.5}{18.5} = 1.11 \quad (13)$$

Where 48 and 27 are the average air side heat transfer coefficient. So that the increment in heat gain should be 11 %, which is not so differ for the 10 %. Therefore, the 77 % heat transfer coefficient ratio is correct. In summary, with using the microchannel condenser, the increment in air side heat transfer coefficient is accompanied by a decrement in convection area and temperature difference so that the difference ratio of heat transfer rate is not so large.

Figure 9 shows that the microchannel condenser cycle has 9 % lower discharge pressure than the conventional one because of the higher heat rejection in the microchannel condenser.

The discharge pressure, whenever it rises, resulting in significant impacts on the refrigeration cycle. the most two important effects are, the higher compressor work that is needed to accomplish the compression, and the lower refrigeration effect. Because, the higher work is needed since the difference between inlet and outlet entropies will be larger. In other word, the compressor should spend more power to compress the hot gas. Because, this hot gas will have a higher resistance to compression each time with ambient temperature due to higher internal energy inside it. Therefore, the compression process will be harder and more work is required to complete it. Regarding to the lower refrigeration effect, it happens because the enthalpy that leaves the condenser increase with saturation temperature or pressure. So, the refrigeration effect will be lower since the same leaving enthalpy will enter the evaporator. Finally, because of the COP is the ratio of refrigeration effect to specific compressor work, it will decrease with the higher pressure, or, in a different expression, the higher ambient temperature.

Now, due to all the above, and since the microchannel cycle has lower discharge pressure, it has about 20 % higher COP than the conventional cycle, as shown in Figure 10. Also, the lower discharge pressure in it leads to 10 % lower compressor work as shown in Figure 11, and 7 % higher refrigeration effect as shown in Figure 12.

5. Conclusions

In this study, the conventional finned tube condenser of the automotive air conditioning cycle is replaced with a microchannel condenser. In order to test whether the microchannel condenser can improve the cycle

performance especially at the high ambient temperature. The study is carried out experimentally for both cycles (the conventional cycle and the microchannel cycle). However, the heat transfer areas of the two condensers isn't the same as already shown in Table 4. This case is due to manufacturing limitation regarding the microchannel con-denser. Now, the upcoming conclusions have been reached

1. The microchannel condenser has 224 % and 77 % higher refrigerant side and air side heat transfer coefficients respectively than the conventional round tube condenser.
2. The heat rejection increased by only 5 % due to 63 % and 20 % reduction in internal and external convection areas with using the microchannel condenser.
3. The microchannel condenser can reduce the space requirement for installation since it has 50 % smaller volume than the conventional round tube condenser.

The microchannel condenser cycle has 9 % lower discharge pressure, 20 % higher COP, 10 % lower work, 10 % higher heat absorption and 7 % higher isentropic efficiency than the conventional cycle.

References

- [1] S. G. Kandlikar and W. J. Grande, "Evolution of microchannel flow passages – Thermohydraulic performance and fabrication technology," *ASME Int. Mech. Eng. Congr. Expo.*, pp. 1–13, 2002.
- [2] S. S. Mehendale, A. M. Jacobi, and R. K. Shah, "Fluid Flow and Heat Transfer at Micro- and Meso-Scales With Application to Heat Exchanger Design," *Appl. Mech. Rev.*, vol. 53, no. 7, p. 175, 2000.
- [3] M. R. K. Satish G. Kandlikar, Srinivas Garimella, Dongqing Li, Stéphane Colin, *Heat transfer and fluid flow in minichannels and microchannels*. 2006.
- [4] M. Ohadi, K. Choo, S. Dessiatoun, and E. Cetegen, *Next Generation Microchannel Heat Exchangers*. 2013.
- [5] C. Y. Park and P. Hrnjak, "Experimental and numerical study on microchannel and round-tube condensers in a R410A residential air-conditioning system," *Int. J. Refrig.*, vol. 31, no. 5, pp. 822–831, 2008.
- [6] M. M. Shah, "Heat Transfer During Condensation Inside Small Channels: Applicability of General Correlation for Macrochannels," *14th Int. Heat Transf. Conf.*, no. 1, pp. 1–10, 2010.
- [7] M. M. Shah, "An Improved and Extended General Correlation for Heat Transfer During Condensation in Plain Tubes," *ASHRAE*, vol. 15, no. 5, pp. 889–914, 2009.
- [8] H. S. Wang and J. W. Rose, "Theory of heat transfer during condensation in microchannels," *Int. J. Heat Mass Transf.*, vol. 54, no. 11–12, pp. 2525–2534, May 2011.
- [9] S. M. Kim and I. Mudawar, "Theoretical model for annular flow condensation in rectangular microchannels," *Int. J. Heat Mass Transf.*, vol. 55, no. 4, pp. 958–970, 2012.
- [10] S. Kim and I. Mudawar, "Universal approach to predicting heat transfer coefficient for condensing mini / micro-channel flow," *Int. J. Heat Mass Transf.*, vol. 56, no. 1–2, pp. 238–250, 2013.
- [11] E. Al-Hajri, A. H. Shooshtari, S. Dessiatoun, and M. M. Ohadi, "Performance characterization of R134a and R245fa in a high aspect ratio microchannel condenser," *Int. J. Refrig.*, vol. 36, no. 2, pp. 588–600, 2013.
- [12] G. Goss and J. C. Passos, "Heat transfer during the condensation of R134a inside eight parallel microchannels," *Int. J. Heat Mass Transf.*, vol. 59, pp. 9–19, Apr. 2013.
- [13] G. Goss, J. L. G. Oliveira, and J. C. Passos, "Pressure drop during condensation of R-134a inside parallel microchannels," *Int. J. Refrig.*, vol. 56, pp. 114–125, Aug. 2015.
- [14] L. Huang, V. Aute, and R. Radermacher, "A model for air-to-refrigerant microchannel condensers with variable tube and fin geometries," *International Journal of Refrigeration*, vol. 40, pp. 269–281, 2014.
- [15] X. Yin, W. Wang, V. Patnaik, and J. Zhou, "Evaluation of microchannel condenser characteristics by numerical simulation," *Int. J. Refrig.*, vol. 54, pp. 126–141, 2015.
- [16] G. F. Nellis and S. a. Klein, *Heat Transfer*. 2009.
- [17] J. . Holman, *Heat Transfer*. 2010.

Table 1. Test Rig General Specifications

<i>Parameter</i>	<i>Specifications</i>
Manufacturer company	Prodit Engineering – Italy
Type	GR030/000/009D
Serial number	6331/0000/000÷6355/0000/000
Manufacturing year	2003
Net weight	84 kg
Gross weight	180 kg
Dimensions	580×610×1400 mm
Working fluid	R134a

Table 2. Microchannel condenser Specifications

<i>Parameters</i>	<i>Specification</i>
Material	Aluminum
Tube arrangement	Parallel
Height	395 mm
Length	431 mm
Depth	25.4 mm
Hydraulic diameter	0.1 mm
Tube cross section	Rectangle
Tube thickness	0.4 mm
Fin material	Aluminum
Fin configuration	Corrugated sheets
Fin thickness	0.1 mm
Fin pitch	2.2 mm
Refrigerant	R22, R134a
Manufactured company	YiWu ShuangChuang Refrigeration equipment Co, Ltd
Serial number	MC-2501-900

Table 3. Conventional round tube condenser specifications

<i>Parameters</i>	<i>Specifications</i>
Height	330 mm
Width	330 mm
Length in air flow direction	90 mm
Outside diameter	10 mm
Inside diameter	8 mm
Tube wall thickness	1 mm
Fin thickness	0.08 mm
Fin pitch	2.08 mm
Vertical distant between tubes	15.7 mm
Horizontal distant between tubes	33.6 mm
Number of rows	4
Number of tubes per row	26
Number of fins	150
Fan diameter	280 mm

Table 4. The two condensers areas

<i>Parameter</i>	<i>Conventional</i>	<i>Microchannel</i>
Dimensions	330 x 330 x 90 mm	395 × 431 × 25.4 mm
Face area	0.1089 m ²	0.17 m ²
Number of fins	150	42
Fin area	0.05532 m ²	0.17 m ²
Total surface area	8.942 m ²	7.14 m ²
Internal convention area	0.2156 m ²	0.08 m ²
Internal cross-sectional area	0.503x10 ⁻⁴ m ²	0.254x10 ⁻⁴ m ²

Table 5. Range of operational conditions

<i>Parameter</i>	<i>Range</i>
Ambient temperature	40-65 °C, $\Delta T = 5$ °C
Discharge pressure	14- 28 bar
Suction pressure	5-6 bar
Saturation temperature	53- 84 °C
Condenser air speeds	8.5 m/s
Indoor temperature	23 °C
Cooling load	2200 W
The cooled space dimensions	580 x 610 x 300 mm
Refrigerant mass flow rate	0.02 kg/s
Refrigerant mass flux	200 kg/m ² s; for conventional cycle 787 kg/m ² s; for microchannel cycle

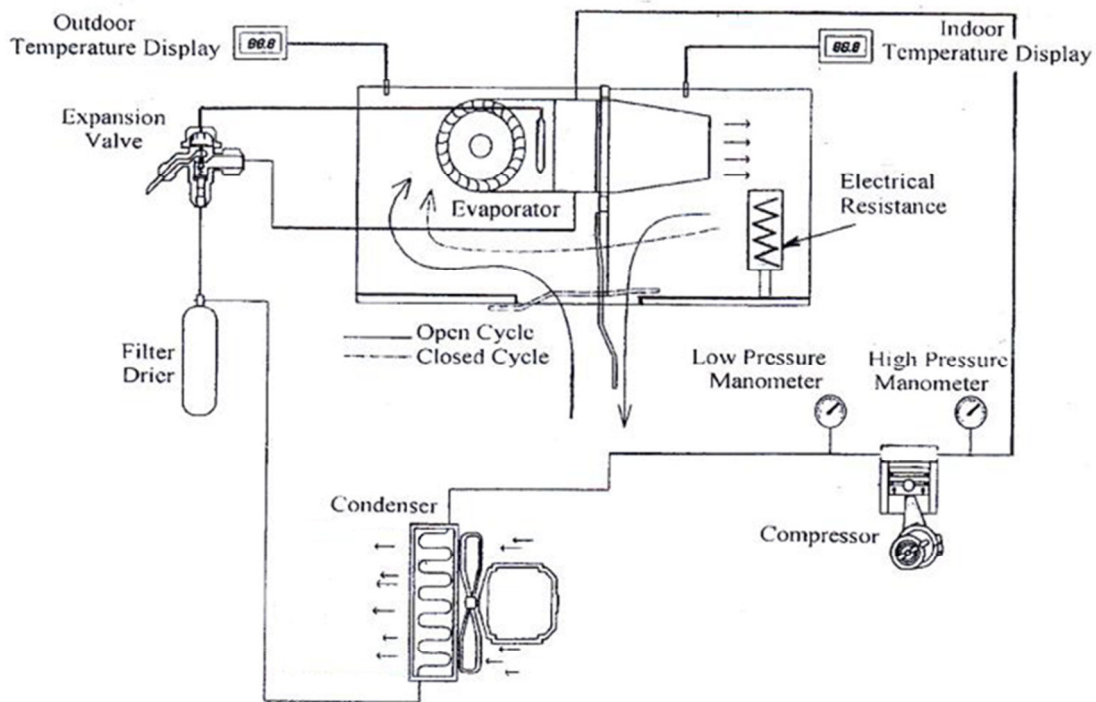


Figure 1: Schematic Diagram of the Test Rig



Figure 2.a: Conventional round tube condenser



Figure 2.b: Microchannel condenser
Figure 2: Photograph of the two condensers

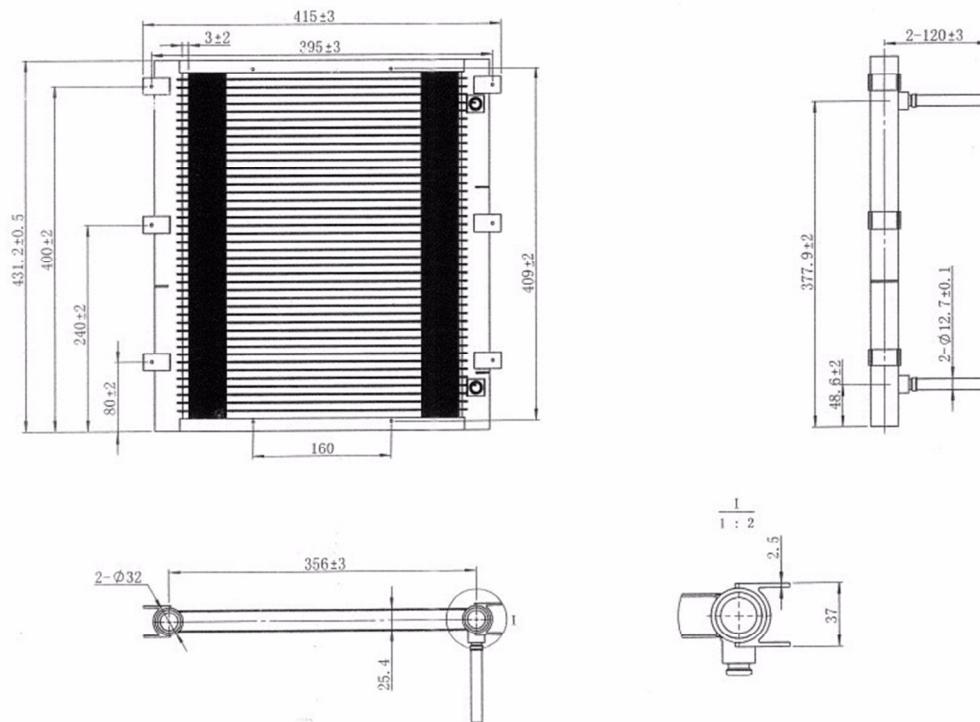


Figure 3: Geometrical diagram of microchannel condenser

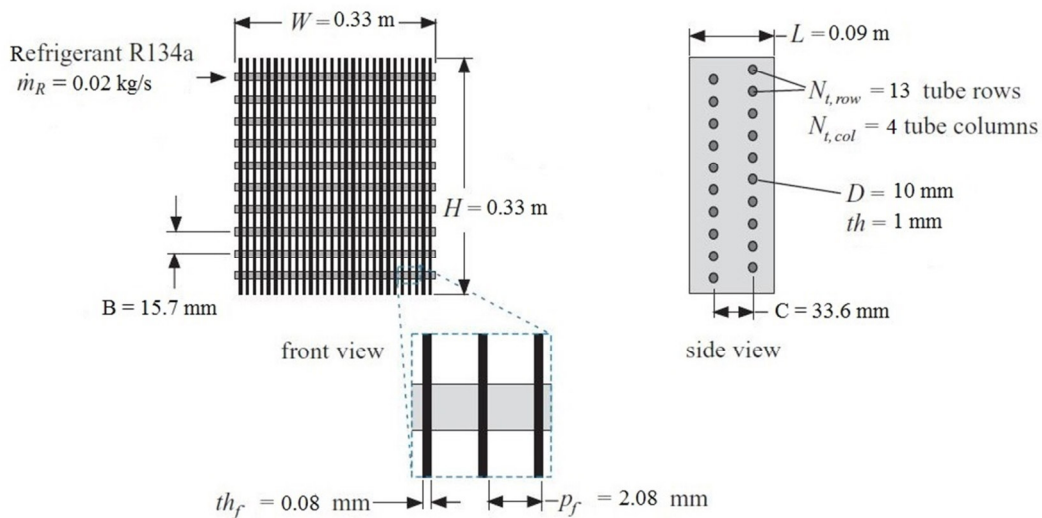


Figure 4: Geometrical diagram of conventional condenser

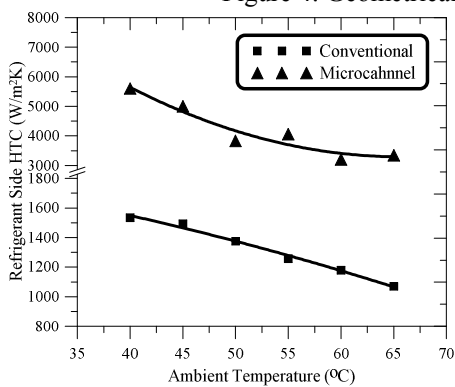


Figure 5: Refrigerant Side HTC Vs. Ambient Temperature

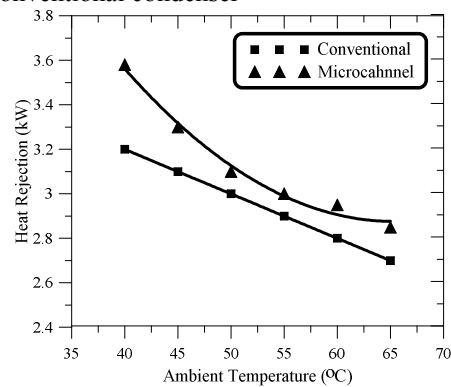


Figure 6 Heat Rejection Vs. Ambient Temperature

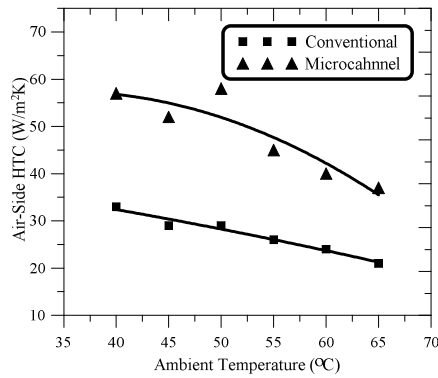


Figure 7: Air Side HTC Vs. Ambient Temperature

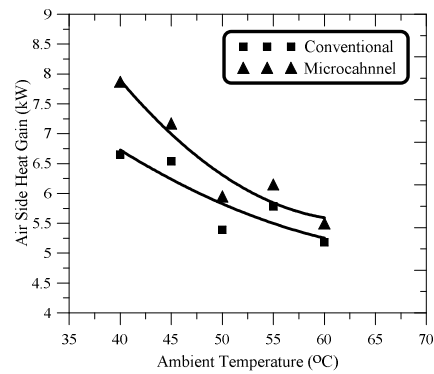


Figure 8: Air Side Heat Gain Vs. Ambient Temperature

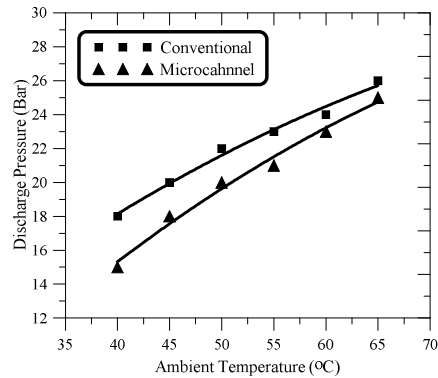


Figure 9: Discharge Pressure Vs. Ambient Temperature

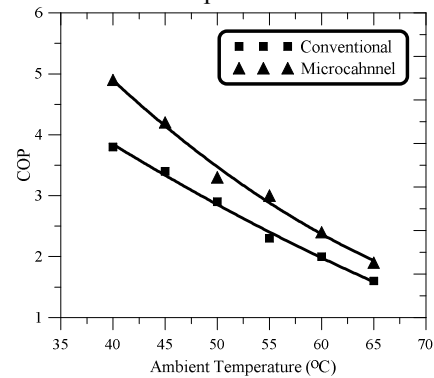


Figure 10: COP Vs. Ambient Temperature

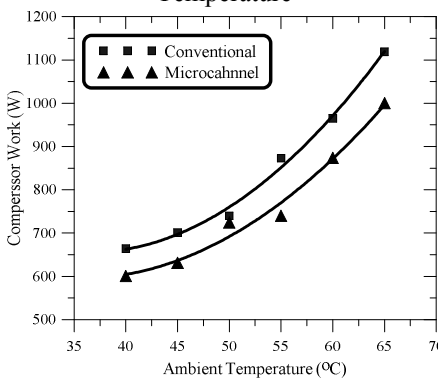


Figure 11: Compressor Work Vs. Ambient Temperature

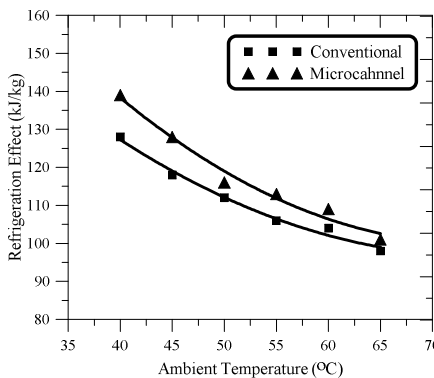


Figure 12: Refrigeration Effect Vs. Ambient Temperature